CrossMark

ORIGINAL ARTICLE

Hypoxia Enhances Tumor-Stroma Crosstalk that Drives the Progression of Hepatocellular Carcinoma

Yuri Cho[1,2] · Eun Ju Cho[1] · Jeong-Hoon Lee[1] · Su Jong Yu[1] · Yoon Jun Kim[1] ·
Chung Yong Kim[1] · Jung-Hwan Yoon[1]

Abstract

Background Crosstalk between tumor cells and their microenvironment plays a crucial role in the progression of hepatocellular carcinoma (HCC). Hypoxia, a common feature of advanced HCC, has been shown to modulate the evolution of the tumor microenvironment. In this study, we investigated the effect of hypoxia on tumor-stroma crosstalk in HCC.
Methods Human HCC cell lines (Huh-BAT, SNU-475) were cocultured with an activated human hepatic stellate cell line (HSCs; LX-2) under either normoxic or hypoxic conditions. Cell growth was evaluated with the MTS assay. Apoptotic signaling cascades were assessed by immunoblot analysis. Expression of CD31 and phosphorylated (p-) Akt in HCC tissues was detected by immunohistochemistry.
Results Coculturing HCC cells with HSCs under hypoxic conditions enhanced their proliferation, migration, and resistance to bile acid (BA)-induced apoptosis compared to coculturing under normoxic conditions. Under hypoxia, of various HSC-derived growth factors, PDGF-BB was the most up-regulated, leading to the activation of the phosphatidylinositol 3-kinase (PI3K)/Akt pathway in HCC cells. Immunohistochemical study also revealed that p-Akt was highly expressed in hypoxic, hypovascular HCC as compared to hypervascular HCC. Neutralizing antisera to PDGF-BB or a PI3K inhibitor attenuated the proliferation of HCC cells cocultured with HSCs, and sensitized HCC cells to BA-induced apoptosis, especially under hypoxic conditions.
Conclusions In conclusion, hypoxic HSC-derived PDGF-BB stimulates the proliferation of HCC cells through activation of the PI3K/Akt pathway, while the inhibition of PDGF-BB or PI3K/Akt pathways enhances apoptotic cell death. Targeting tumor-stroma crosstalk might be a novel therapy in the management of human HCCs.

Yuri Cho and Eun Ju Cho have contributed equally to this work.

✉ Jung-Hwan Yoon
  yoonjh@snu.ac.kr

  Yuri Cho
  presh_yuri@hanmail.net

  Eun Ju Cho
  creatioex@gmail.com

  Jeong-Hoon Lee
  pindra@empal.com

  Su Jong Yu
  ydoctor2@hanmail.net

  Yoon Jun Kim
  yoonjun@snu.ac.kr

  Chung Yong Kim
  aja2013@hanmail.net

[1] Department of Internal Medicine and Liver Research Institute, Seoul National University College of Medicine, 101 Daehak-ro, Jongno-gu, Seoul 03080, Republic of Korea

[2] Department of Internal Medicine, CHA Gangnam Medical Center, CHA University, Seoul, Republic of Korea

Abbreviations

HCC	Hepatocellular carcinoma
HSC	Hepatic stellate cell
MTS	3-(4,5-Dimethylthiazol-2-yl)-5-(3-carboxy-methoxyphenyl)-2-(4-sulfophenyl)-2H-tetrazolium
DAPI	4′,6-Diamidino-2-phenylindole
BA	Bile acid
ELISA	Enzyme-linked immunosorbent assay

RT-PCR	Reverse transcription-polymerase chain reaction
Akt	Protein kinase B
PTEN	Phosphatase and tensin homolog
PI3K	Phosphoinositide 3-kinase
PDGF	Platelet-derived growth factor
FGF	Fibroblast growth factor
TGF	Transforming growth factor
CTGF	Connective tissue growth factor
MAPK	Mitogen-activated protein kinase
OD	Optical density
SD	Standard deviation
IHC	Immunohistochemical
FOXO	Forkhead transcription factors

Introduction

Hepatocellular carcinoma (HCC) is one of the most fatal of cancers with an increasing global incidence [1]. The majority of HCC patients are treated for chronic liver disease or liver cirrhosis (LC), both of which are major risk factors for the development of HCC [2].

A remodeling of the microenvironment of liver in the patients with chronic liver disease or LC is a hallmark of HCC [3]. It is well known that activation of hepatic stellate cells (HSCs) plays a vital role in the development of hepatic fibrosis. In addition, crosstalk between HCC cells and the surrounding microenvironment is believed to play a pivotal role in modulating the biological behavior of the tumor [4, 5]. During chronic liver damage, HSCs become activated and assume a myofibroblast-like phenotype. These cells proliferate and migrate towards the area of ongoing tissue remodeling and secrete extracellular matrix proteins [6]. Moreover, the stroma of the HCC is infiltrated by both activated HSCs and myofibroblasts. The interaction between them affects HCC development by triggering cell proliferation and survival of surrounding tissues [4, 7].

Hypoxia induces survival in HCC by activating a variety of growth factor signals. Hypoxia stimulates angiogenesis by hypoxia-inducible factor-1 (HIF-1), vascular endothelial growth factor (VEGF), basic fibroblast growth factor (bFGF), and angiopoietin-1 (ANG-1) [8]. In addition, hypoxia stimulates HCC cell proliferation by inducing transforming growth factor-β (TGF-β) and platelet derived growth factor (PDGF), facilitates glycolysis by up-regulating hexokinase-II expression [9, 10], induces the immortalization of HCC cells by activating telomerase and histone deacetylase [11], and inhibits cellular apoptosis by inducing the inhibitor of apoptosis protein-2 (IAP-2) and myeloid cell factor-1 (Mcl-1) [12]. Therefore, under hypoxic conditions, the microenvironment may undergo dramatic changes mediated by various cytokines and growth factors, which lead to tumor growth, and metastasis.

However, the molecular mechanisms involved, and the consequences of any crosstalk between tumor cells and activated HSCs, especially under hypoxic conditions, remain largely unknown [13]. The current study investigated the effects of hypoxia on tumor-stroma crosstalk in HCC.

Methods

Cell Lines and Coculture

Human HCC cell lines and a hepatic stellate cell line were used in this study: Huh-BAT, a well-differentiated, bile acid transporter-transfected HCC cell line [14]; SNU-475, a poorly differentiated HCC cell line [15]; and LX-2, an activated, human HSC line [16]. Cells were grown in Dulbecco's Modified Eagle Medium (DMEM, Huh-BAT, and LX-2) or in RPMI 1640 (SNU-475) supplemented with 10 % fetal bovine serum (FBS), 100,000 U/L penicillin, and 100 mg/L streptomycin, with or without 100 nM insulin. Coculture experiments were performed in serum-free DMEM or RPMI 1640 using 1-μm pore size transwell inserts (Corning; Lowell, MA, USA). Transwell inserts permitted diffusion of media; however, they prevented cell migration. HCC and LX-2 cell lines were incubated alone, or side-by-side, using transwell inserts under either standard (20 % O_2 and 5 % CO_2, at 37 °C) or hypoxic (1 % O_2, 5 % CO_2, and 94 % N_2, at 37 °C) culture conditions.

Cell Proliferation Analysis

Cell growth was measured colorimetrically using a Cell-Titer 96® AQueous One Solution Cell Proliferation Assay (Promega Corporation; Madison, WI, USA). Briefly, this assay requires cellular conversion of 3,4-(5-dimethylthia-zol-2-yl)-5-(3-carboxymethoxyphenyl)-2-(4-sulfophenyl)-2H-tetrazolium salt (MTS) into soluble formazan by dehydrogenase enzymes produced only by metabolically active, proliferating cells. Following each treatment, 20 μL of CellTiter 96® AQueous One Solution reagent was added to each well of a 96-well plate. After an 1 h incubation, the absorbance of each well was measured at a 490 nm wavelength using an ELISA plate reader (Molecular Devices; Sunnyvale, CA).

Migration Assay

Migration was assessed by using a time-lapse scratch assay (wound-healing-assay). Briefly, HCC cells were seeded at high density into 6-well plates. Following adherence, cells were washed with serum-free DMEM and incubated in either control medium or medium derived from activated HSCs. The cell layer was scratched with a pipette tip and the degree of cell migration measured after 24 and 48 h. Each analysis was performed in triplicate and repeated three times.

Apoptosis Analysis

Chromatic condensation and nuclear fragmentation were assessed using a DNA binding dye, 40,6-diamidino-2-phenylindole dihydrochloride (DAPI), and fluorescence microscopy (Carl Zeiss; Jena, Germany).

Quantification of Growth Factors

The mRNA expressions of human fibroblast growth factor 10 (FGF10), fibroblast growth factor 5 (FGF5), connective tissue growth factor (CTGF), transforming growth factor-ß1 (TGF-ß1), and platelet-derived growth factor beta polypeptide (PDGF-B) were assessed using a real-time reverse-transcriptase polymerase chain reaction (RT-PCR). Total ribonucleic acids (RNAs) were extracted from cells using Trizol Reagent (Invitrogen, Carlsbad, CA). Complementary deoxyribonucleic acid (cDNA) templates were prepared using oligo(dT) random primers and Moloney Murine Leukemia Virus (MoMLV) reverse transcriptase. After the reverse transcription reaction, the cDNA template was amplified by PCR using Taq polymerase (Invitrogen). Relative quantification was calculated using the $2^{-\Delta\Delta C_T}$ method, with GAPDH as the internal control. All PCR experiments were performed in triplicate. In addition, the amount of PDGF-BB in cell culture supernatants was assessed by an ELISA kit (R&D Systems; Abingdon, UK).

Immunoblot Assay

Antibodies against: caspase-9, caspase-8, cleaved caspase-7, PDGFR-β, phosphorylated (p-) PDGFR-β (Tyr 751), total Akt, p-Akt (Ser473), total phosphatase and tensin homolog deleted on chromosome ten (PTEN), p-PTEN (Ser380/Thr382/383), total-p42/44 (Thr202/Tyr204), p-p42/44, p-p38 (Thr180/Tyr182), total Forkhead transcription factor (FOXO)3a, and p-FOXO3a were purchased from Cell Signaling (Beverly, MA, USA). Cells were lysed for 20 min on ice using lysis buffer (50 mM Tris–HCl, pH 7.4; 1 % Nonidet P-40; 0.25 % sodium deoxycholate; 150 mM NaCl; 1 mM EDTA; 1 mM phenylmethylsulfonylfluoride; aprotinin, leupeptin, and pepstatin (1 µg/mL each); 1 mM Na_3VO_4; and 1 mM NaF) and centrifuged at $14,000 \times g$ for 15 min at 4 °C. Samples were resolved by sodium dodecyl sulfate polyacrylamide gel electrophoresis, transferred to nitrocellulose membranes, blotted with the appropriate primary antibodies, and incubated with peroxidase-conjugated secondary antibodies (Biosource International; Camarillo, CA). Bound antibodies were visualized using a chemiluminescent substrate (ECL; Amersham; Arlington Heights, IL) and exposed to Kodak X-OMAT film. The images were detected using an image analyzer (LAS-1000, Fuji Photo Film, Tokyo, Japan), and densitometric analyses were performed using ImageJ software (National Institutes of Health, Bethesda, MD).

Immunohistochemical Study

Four representative human hypervascular and hypovascular HCC tissues used in our previous study were analyzed [17]. Tumor vascularity was assessed according to the arterial enhancement patterns on dynamic computed tomography (CT) and vascular appearance at the tissue by CD31 immunohistochemical (IHC) staining. IHC was performed according to the manufacturer's protocol using the anti-mouse CD31 antibody (Vector Laboratories, Inc., Burlingame) at a 1:200 dilution or anti-rabbit-p-Akt antibody (Cell Signaling, Beverly, MA) at 1:100 dilution [18]. The study protocol was reviewed and approved by the Institutional Review Board of Seoul National University Hospital (IRB No. 1003-099-314).

Data Analysis

All experimental results were acquired from three independent experiments and are presented as mean ± standard deviation (SD). Comparisons between groups were analyzed using the Mann–Whitney U test and $P < 0.05$ was considered statistically significant. All analyses were conducted using SPSS version 22.0 (SPSS Inc.; Chicago, IL, USA).

Results

Enhanced Cell Proliferation and Migration by Coculturing in Hypoxia

Initially, we examined whether coculturing HCC cells with HSCs under hypoxic conditions could modulate the proliferation and migration of cells. Compared with HCC cells (Huh-BAT or SNU-475) cultured alone, coculturing with LX-2 cells significantly increased the proliferation of HCC

cells, which was further augmented under hypoxic conditions (Fig. 1). In addition, coculturing HCC cells with LX-2 cells under hypoxia significantly accelerated the migration of HCC cells compared with coculturing under normoxia (Fig. 2).

Decreased Bile Acid-Induced HCC Cell Apoptosis

Next, we evaluated the effect of coculture conditions on cellular apoptosis. As reported previously, hypoxia enhances resistance to bile acid (BA)-induced apoptosis [10]. Huh-BAT cells cocultured with LX-2 cells were significantly more resistant to BA-induced HCC cell

apoptosis compared to monocultured cells, especially under hypoxic conditions (Fig. 3a). Western blot analyses confirmed that coculturing with LX-2 cells attenuated BA-induced activation of caspase-9, -8 and -7 in Huh-BAT cells, under hypoxic conditions (Fig. 3b).

The Effects of Hypoxic HSC-Derived PDGF-BB on HCC Cells

We evaluated mRNA expression of HSC-derived, HCC-relevant growth factors such as TGF-β1, FGF5 and 10, CTGF, and PDGF-B in LX-2 cells (Fig. 4a). Among the growth factors tested, PDGF-B exhibited the most
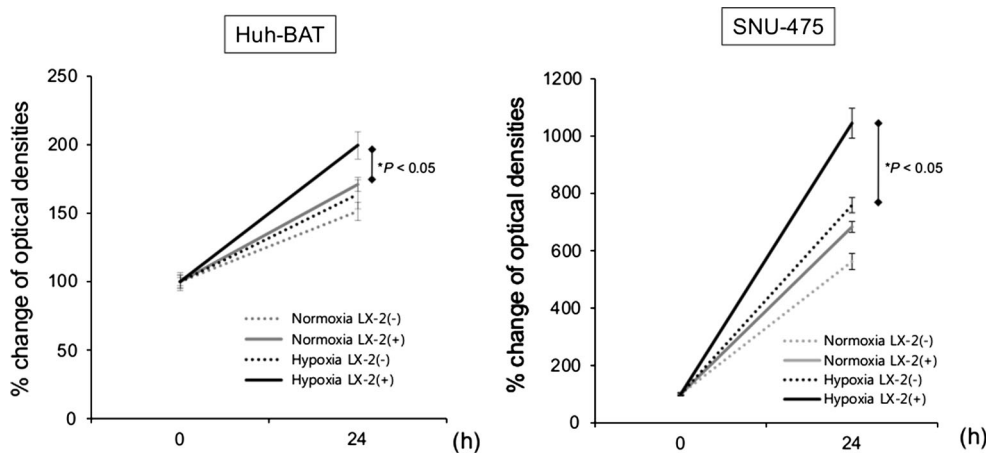

Fig. 1 Coculturing with HSCs under hypoxic conditions accelerated HCC cell proliferation. HCC cells (Huh-BAT, SNU-475) were monocultured or co-cultured with HSCs (LX-2), either in normoxic (20 % O_2 and 5 % CO_2; at 37 °C) or hypoxic (1 % O_2, 5 % CO_2, and 94 % N_2; at 37 °C) conditions. At each indicated time point, MTS assays were performed. Data are expressed as mean ± SD of percent changes of triplicate optical densities compared to time 0 (*$P < 0.05$, vs. coculturing under normoxic conditions)
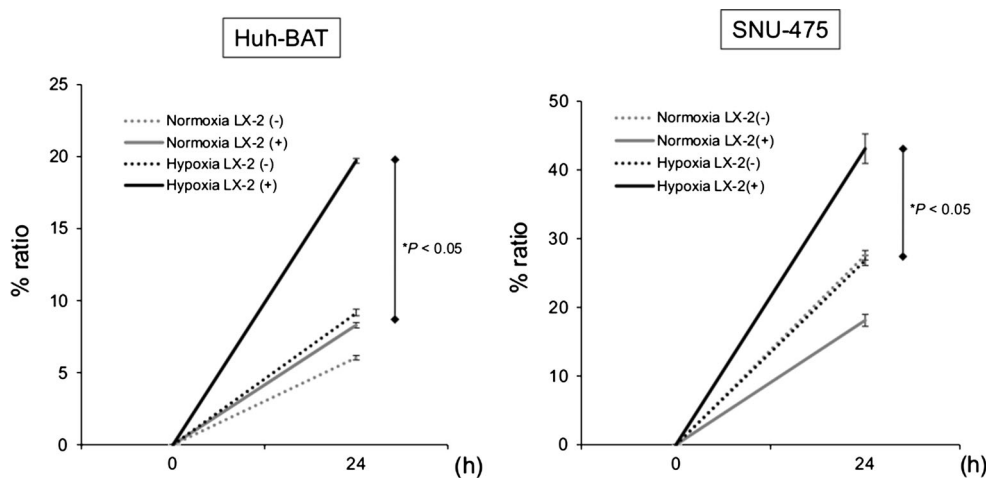

Fig. 2 Conditioned medium derived from coculturing of HCC cells and HSCs under hypoxia enhanced HCC cell migration. HCC cells (Huh-BAT, SNU-475) were seeded at high density into 6-well plates. Following adherence, the cell layer was scratched with a pipette tip, and cells were cultured in conditioned medium derived from HCC cells monocultured or cocultured with LX-2, either under normoxic or hypoxic conditions. The degree of cell migration was measured after 24 and 48 h. Data are expressed as mean ± SD of percent changes compared to time 0 (*$P < 0.05$, vs. coculturing under normoxic conditions). The experiment was repeated three times
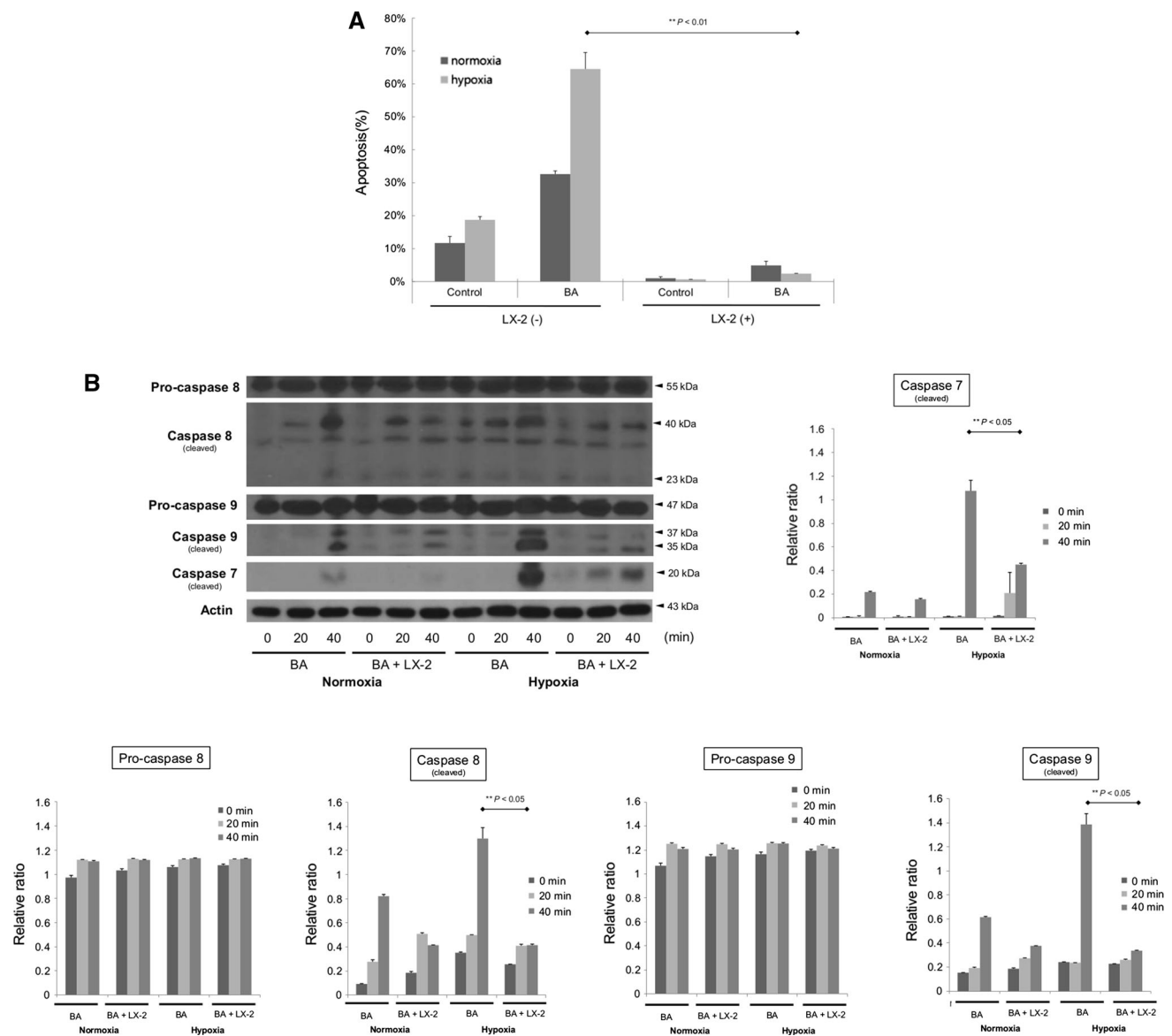
Fig. 3 Coculturing with HSCs under hypoxia decreased bile acid-induced HCC cell apoptosis. **a** Huh-BAT cells were monocultured or cocultured with LX-2, either under normoxic or hypoxic conditions. After 24 h, cells were treated with deoxycholate (300 μM) for 2 h. Apoptosis was assessed using DAPI staining and fluorescence microscopy. Data are expressed as mean ± SD from three different experiments (**$P < 0.01$, vs. mono-culturing without LX-2). The experiment was repeated three times. **b** Immunoblot analyses were performed on the lysates of Huh-BAT cells treated as in **a** for each indicated time period. Results of densitometric analysis are presented as the mean ± SD of the relative ratio of cleaved caspase-7, 8, 9 or procaspase-8, 9 to β-actin. The experiment was repeated three times

significant fold-change in mRNA expression levels under hypoxic conditions. Furthermore, LX-2 cells secreted significantly higher levels of PDGF-BB protein under hypoxic conditions (Fig. 4b).

To evaluate whether PDGF-BB can reproduce the cytoprotective effects of hypoxic coculture condition on HCC cells, Huh-BAT cells were treated with exogenous PDGF-BB under normoxic conditions. PDGF-BB significantly enhanced proliferation (Fig. 5a) and migration of Huh-BAT cells (Fig. 5b).

In addition, PDGF-BB protected HCC cells from BA-induced apoptosis (Fig. 5c), especially under hypoxic conditions. When Huh-BAT cells were treated with neutralizing antiserum to PDGF-BB, the proliferation of cocultured cells under hypoxia significantly decreased compared to the proliferation of cocultured cells under normoxia (Fig. 5d). Anti-PDGF-BB also sensitized Huh-BAT cells to BA-induced apoptosis, especially under hypoxic conditions (Fig. 5e). These results suggest HSC-derived PDGF-BB promotes proliferation and resistance to

apoptosis of HCC cells, especially under hypoxic conditions.

In response to the upregulation of PDGF-BB, phosphorylation of PDGFR-β was enhanced in Huh-BAT cells cocultured with LX-2 cells under hypoxia (Fig. 6a). Given that Ras-p42/44 mitogen-activated protein kinase (MAPK) pathways and the phosphatidylinositol 3-kinase (PI3K)/Akt pathway are important downstream pathways of PDGFR-β, we evaluated the expression of p-p42/44 and p-Akt. As shown in Fig. 6b, coculturing with LX-2 cells under hypoxic conditions augmented the activation of Akt and p42/44 in Huh-BAT cells. Akt-dependent phosphorylation of FOXO3a was also up-regulated. In contrast, the expression levels of p-p38, total Akt, total PTEN, and p-PTEN were not affected. When Huh-BAT cells were treated with PI3K inhibitor (LY294002), the proliferation of cocultured cells under hypoxia significantly decreased compared to that under normoxia (Fig. 6c), whereas p42/44 inhibitor (U0126) did not significantly affect cell proliferation.

IHC study using human HCC tissues also revealed that p-Akt was highly expressed in hypoxic, hypovascular HCC as compared to hypervascular HCC (Fig. 7). Taken together, these findings suggest that hypoxic HSC-derived PDGF-BB promotes HCC progression, mainly via activation of the PI3K/Akt pathway.

Discussion

HCC cells under hypoxic conditions generally show more rapid proliferation than cells with an adequate vascular supply [19]. It has been reported that HSCs play a critical role in HCC tumor progression, as the presence of HSCs in peritumoral tissue is associated with strong vascular invasion and aggressive pathological characteristics [20]. However, the manner in which HSCs modulate the invasive HCC phenotype, particularly under hypoxic conditions, remains unclear.

In the present study, activated HSCs induced the proliferation and migration of HCC cells, and suppressed BA-induced HCC cell apoptosis, particularly under hypoxic conditions. The anti-proliferative effects of PI3K inhibitor on HCC cells cocultured with HSCs were more prominent under hypoxic conditions, indicating that the PI3K/Akt pathway may be implicated in tumor progression under hypoxic conditions, more so than tumor progression under normoxic conditions. Akt-dependent inhibitory phosphorylation of FOXO3a was also up-regulated under hypoxia, which may lead to HCC cell survival.

The PI3K/Akt pathway is a well-known, promising target for the treatment of HCC, which has its pivotal role in regulating cell proliferation, migration, survival, and angiogenesis. Dysregulation of PI3K/Akt pathway in HCC has been frequently documented [21]. Furthermore, the PI3K/Akt pathway also induces the activation and proliferation of HSCs, leading to the development of fibrosis and HCC in PDGF-C transgenic mice [22], suggesting that this molecular pathway may be critical in hepatocarcinogenesis. Similarly, our results suggest that the PI3K/Akt pathway is crucial in proliferation and invasion of HCC, especially under hypoxic conditions.

PGDF consists of two related peptide chains, PDGF-A and PDGF-B, which contain intramolecular disulfide bonds linking the subunits. Of the isoforms of PDGF, the PDGF-BB isoform is a mitogen for vascular smooth muscle cells [23], and is one of the key factors involved in hepatocarcinogenesis. A recent study reported that the
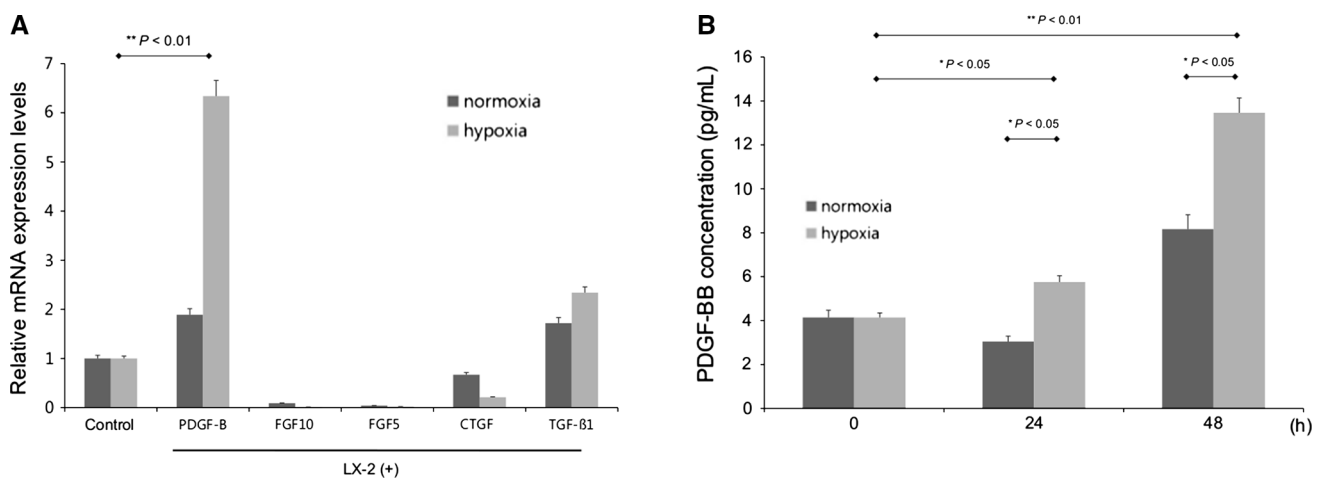

Fig. 4 The expression of PDGF-BB was significantly upregulated in hypoxic HSC. a PDGF-B, FGF10, FGF5, CTGF, and TGFβ1 mRNAs in LX-2 cells cultured under normoxic or hypoxic conditions for 24 h were quantified by RT-PCR and normalized to GAPDH expression levels. The experiment was repeated three times. b LX-2 cells were treated as in a. The amount of PDGF-BB in serum-free supernatant was measured by ELISA, and corrected for total protein expression. Data are expressed as mean ± SD from three different experiments
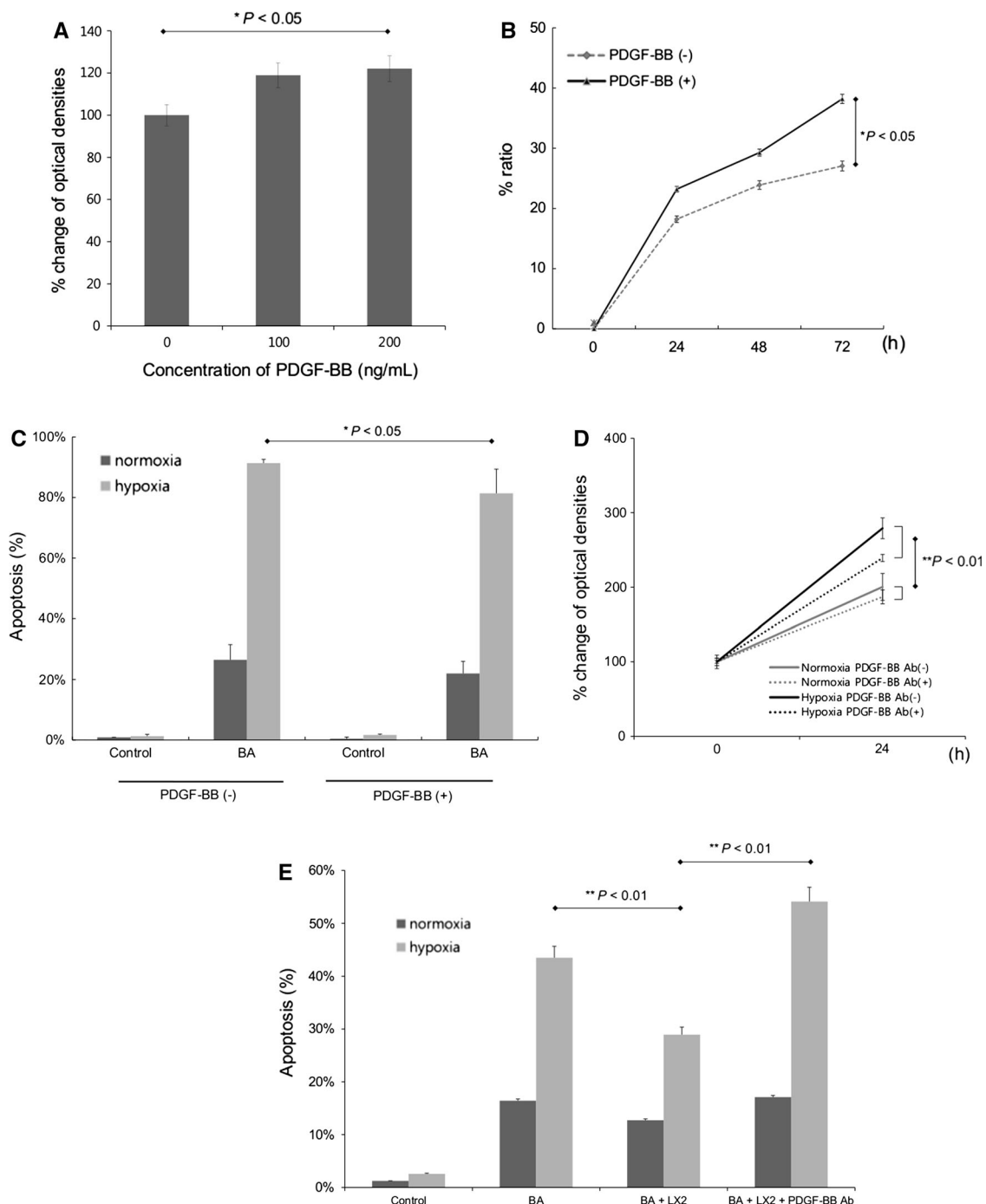
Fig. 5 Hypoxic HSC-derived PDGF-BB is a survival factor for HCC cells. **a** Huh-BAT cells were treated with PDGF-BB at concentrations between 0 and 200 ng/mL under normoxic conditions. After 24 h, a MTS assay was performed. Data are expressed as mean ± SD of percent changes of triplicate optical densities compared to that of control. **b** A migration assay was performed using Huh-BAT cells treated with vehicle or PDGF-BB (200 ng/mL) for the indicated time periods under normoxic conditions. Data are expressed as mean ± SD of percent changes compared to time 0 h. The experiment was repeated three times. **c** Huh-BAT cells were treated with deoxycholate (300 μM) for 2 h following PDGF-BB pretreatment (16 h), either in normoxic or hypoxic conditions. Apoptosis was assessed using DAPI staining and fluorescence microscopy. Data are expressed as mean ± SD from three different experiments

($*P < 0.05$, vs. without PDGF-BB pretreatment). **d** Huh-BAT cells were cocultured with LX-2 cells in the presence or absence of PDGF-BB antibody (10 μg/mL) under normoxic or hypoxic conditions. After 24 h, a MTS assay was performed. Data are expressed as mean ± SD of percent changes of optical densities compared to that of control ($**P < 0.01$, vs. the difference in HCC proliferation according to the presence of absence of PDGF-BB antibody under normoxic conditions). The experiment was repeated three times. **e** Huh-BAT cells were monocultured or cocultured with LX-2 in the presence or absence of PDGF-BB antibody (10 μg/mL) under normoxic or hypoxic conditions. After 40 h, cells were treated with deoxycholate (300 μM) for 2 h. Apoptosis was assessed using DAPI staining and fluorescence microscopy. Data were expressed as mean ± SD from three different experiments

Fig. 6 PDGF-BB-mediated HCC cell growth is dependent on the PI3K/Akt pathway. **a** Huh-BAT cells were monocultured or cocultured with LX-2 either in normoxic or hypoxic conditions for each indicated time period. The expression of p-PDGFR-β was analyzed by immunoblotting cell lysate and densitometric analysis. The experiment was repeated three times. **b** Immunoblot analyses of p-Akt, total Akt, p-PTEN, PTEN, p-p42/44, total p42/44, and p-p38 were performed in cells treated as in **a**. **c** Huh-BAT cells were monocultured or cocultured with LX-2 either under normoxic or hypoxic conditions for 24 h. Cells were further treated with or without PI3K inhibitor (LY294002, 20 μM) or p42/44 inhibitor (U0126, 5 μM) for 40 h, and a MTS assay was performed. Data are expressed as mean ± SD of percent changes of triplicate optical densities compared to control (*$P < 0.05$, vs. the difference in HCC proliferation according to the presence of absence of PI3K inhibitor under normoxic coculturing conditions)
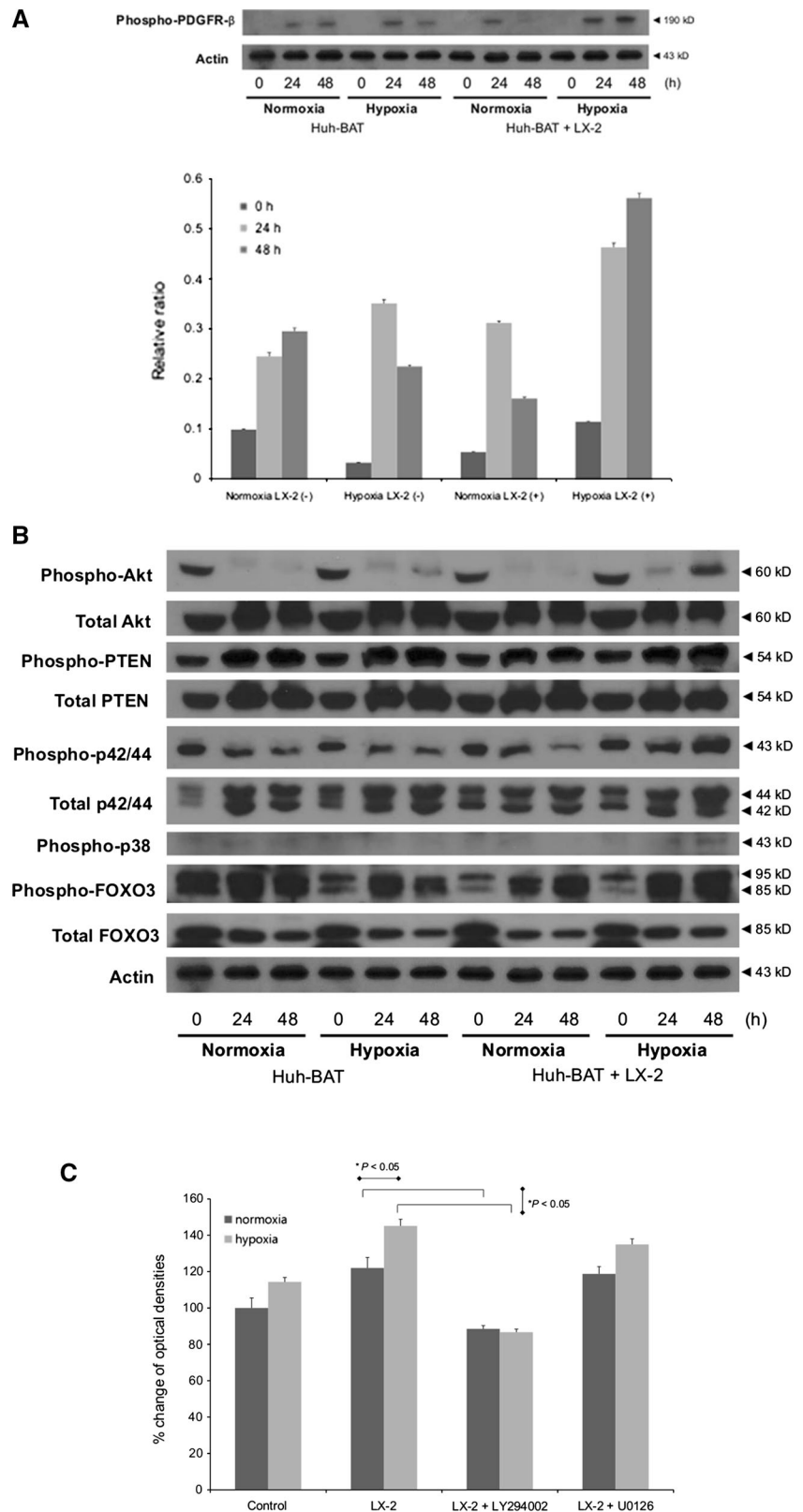
overexpression of PDGF-BB accelerated hepatic fibrosis and chemically induced hepatocarcinogenesis by upregulation of the TGF-β receptor, β-catenin, and vascular endothelial growth factor in transgenic mice [24]. Likewise, exogenous PDGF-BB enhanced proliferation and migration of HCC cells, and protected cells from BA-
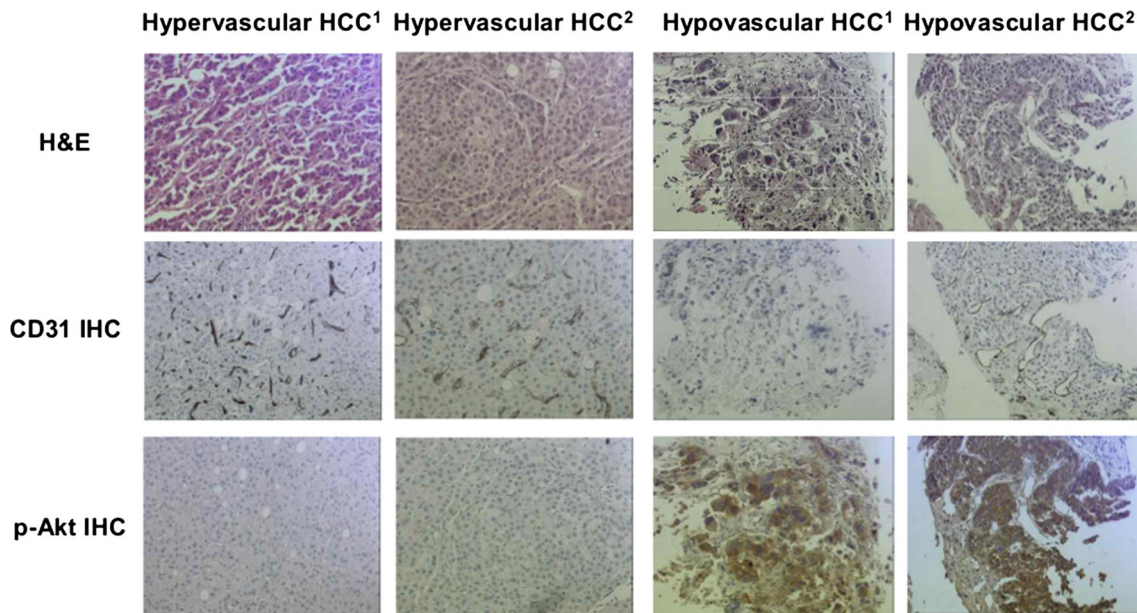
Fig. 7 P-Akt was highly expressed in hypovascular HCC as compared to hypervascular HCC. Expression of CD31 and p-Akt in hypervascular and hypovascular human HCC tissues were detected by immunohistochemistry (×200)

induced apoptosis in our study. In addition, the levels of PDGF-BB derived from HSCs were significantly upregulated under hypoxic conditions, leading to the enhanced activation of PDGFR-β, p42/44 MAPK, and PI3K/Akt pathways in HCC cells. These findings suggest that hypoxic HSC-derived PDGF-BB induces HCC progression through the activation of PI3K/Akt and p42/44 MAPK signaling pathways, as a consequence of tumor-stroma crosstalk under hypoxic conditions. These results further suggest that targeting the PI3K pathway or PDGF receptor may enhance the efficacy of chemotherapeutic agents against HCC in a hypoxic microenvironment.

In conclusion, the current study indicates that hypoxic HSC-derived PDGF-BB stimulates HCC cell proliferation and attenuates BA-induced apoptosis in a PI3K/Akt-signaling-dependent manner. Targeting tumor-stroma crosstalk might be a novel therapy in the management of human HCC.

Compliance with ethical standards

Conflict of interest Authors disclose no conflicts of interest.

References

1. El-Serag HB. Hepatocellular carcinoma: recent trends in the United States. *Gastroenterology*. 2004;127:S27–S34.

2. Bruix J, Boix L, Sala M, Llovet JM. Focus on hepatocellular carcinoma. *Cancer Cell*. 2004;5:215–219.

3. Theret N, Musso O, Turlin B, et al. Increased extracellular matrix remodeling is associated with tumor progression in human hepatocellular carcinomas. *Hepatology*. 2001;34:82–88.

4. Eiro N, Vizoso FJ. Importance of tumor/stroma interactions in prognosis of hepatocellular carcinoma. *Hepatobiliary Surg Nutr*. 2014;3:98–101.

5. Coulouarn C, Clement B. Stellate cells and the development of liver cancer: therapeutic potential of targeting the stroma. *J Hepatol*. 2014;60:1306–1309.

6. Pinzani M, Macias-Barragan J. Update on the pathophysiology of liver fibrosis. *Expert Rev Gastroenterol Hepatol*. 2010;4:459–472.

7. Gupta DK, Singh N, Sahu DK. TGF-beta mediated crosstalk between malignant hepatocyte and tumor microenvironment in hepatocellular carcinoma. *Cancer Growth Metastasis*. 2014;7:1–8.

8. Lee HJ, Kang HJ, Kim KM, et al. Fibroblast growth factor receptor isotype expression and its association with overall survival in patients with hepatocellular carcinoma. *Clin Mol Hepatol*. 2015;21:60–70.

9. Lal A, Peters H, St Croix B, et al. Transcriptional response to hypoxia in human tumors. *J Natl Cancer Inst*. 2001;93:1337–1343.

10. Gwak GY, Yoon JH, Kim KM, Lee HS, Chung JW, Gores GJ. Hypoxia stimulates proliferation of human hepatoma cells through the induction of hexokinase II expression. *J Hepatol*. 2005;42:358–364.

11. Kim MS, Kwon HJ, Lee YM, et al. Histone deacetylases induce angiogenesis by negative regulation of tumor suppressor genes. *Nat Med*. 2001;7:437–443.

12. Stoeltzing O, Ahmad SA, Liu W, et al. Angiopoietin-1 inhibits vascular permeability, angiogenesis, and growth of hepatic colon cancer tumors. *Cancer Res*. 2003;63:3370–3377.

13. Lee JS. The mutational landscape of hepatocellular carcinoma. *Clin Mol Hepatol*. 2015;21:220–229.

14. Nakabayashi H, Taketa K, Miyano K, Yamane T, Sato J. Growth of human hepatoma cells lines with differentiated functions in chemically defined medium. *Cancer Res*. 1982;42:3858–3863.

15. Park JG, Lee JH, Kang MS, et al. Characterization of cell lines established from human hepatocellular carcinoma. *Int J Cancer*. 1995;62:276–282.

16. Xu L, Hui AY, Albanis E, et al. Human hepatic stellate cell lines, LX-1 and LX-2: new tools for analysis of hepatic fibrosis. *Gut*. 2005;54:142–151.

17. Chung GE, Lee JH, Yoon JH, et al. Prognostic implications of tumor vascularity and its relationship to cytokeratin 19 expression in patients with hepatocellular carcinoma. *Abdom Imaging*. 2012;37:439–446.

18. Liang Y, Zheng T, Song R, et al. Hypoxia-mediated sorafenib resistance can be overcome by EF24 through Von Hippel–Lindau tumor suppressor-dependent HIF-1alpha inhibition in hepatocellular carcinoma. *Hepatology*. 2013;57:1847–1857.

19. Tezuka M, Hayashi K, Kubota K, et al. Growth rate of locally recurrent hepatocellular carcinoma after transcatheter arterial chemoembolization: comparing the growth rate of locally recurrent tumor with that of primary hepatocellular carcinoma. *Dig Dis Sci*. 2007;52:783–788.

20. Amann T, Bataille F, Spruss T, et al. Activated hepatic stellate cells promote tumorigenicity of hepatocellular carcinoma. *Cancer Sci*. 2009;100:646–653.

21. Engelman JA. Targeting PI3K signalling in cancer: opportunities, challenges and limitations. *Nat Rev Cancer*. 2009;9:550–562.

22. Campbell JS, Hughes SD, Gilbertson DG, et al. Platelet-derived growth factor C induces liver fibrosis, steatosis, and hepatocellular carcinoma. *Proc Natl Acad Sci USA*. 2005;102:3389–3394.

23. Vaillancourt RR, Gardner AM, Kazlauskas A, Johnson GL. The kinase-inactive PDGF beta-receptor mediates activation of the MAP kinase cascade via the endogenous PDGF alpha-receptor in HepG2 cells. *Oncogene*. 1996;13:151–159.

24. Maass T, Thieringer FR, Mann A, et al. Liver specific overexpression of platelet-derived growth factor-B accelerates liver cancer development in chemically induced liver carcinogenesis. *Int J Cancer*. 2011;128:1259–1268.